Journal of Fluids and Structures 42 (2013) 152–165

Contents lists available at ScienceDirect

Journal of Fluids and Structures

journal homepage: www.elsevier.com/locate/jfs

Studying the coupled eigenoscillations of an axisymmetric tower-elevated tank system by the multimodal method

I. Gavrilyuk [a], M. Hermann [b], Yu. Trotsenko [c], A. Timokha [c,d,*]

[a] University of Cooperative Education, Berufsakademie Eisenach-Staatliche Studienakademie Thüringen, Am Wartenberg 2, D-99817 Eisenach, Germany
[b] Friedrich-Schiller-Universität Jena, Ernst-Abbe-Platz 1-2, Jena D-07745, Germany
[c] Institute of Mathematics, National Academy of Sciences of Ukraine, Tereschenkivska 3, str., 01601, Kiev, Ukraine
[d] Centre for Autonomous Marine Operations and Structures, Norwegian University of Science and Technology, NO-7491 Trondheim, Norway

ARTICLE INFO

Article history:
Received 20 August 2012
Accepted 2 June 2013
Available online 16 July 2013

Keywords:
Sloshing
Water tower
Coupled dynamics
Ritz method

ABSTRACT

Employing the virtual work variational principle and the linear multimodal method for the liquid sloshing in an axisymmetric tank, we study coupled eigenoscillations of a tower and an elevated tank partially filled by a liquid. An emphasis is placed on the case of an upright circular cylindrical tank. Theoretical results are compared with known experimental data.

1. Introduction

Studying water tower dynamics is an important task of civil engineering. The supporting structure (tower) typically has a complex design and can be considered as either a reinforced frame type staging configuration (Dutta et al., 2004) or an orthotropic shell equipped by various internal stingers, stiffeners, and webs. When the tower height is much larger than the horizontal tower dimension, the structural vibrations can be described within the framework of the beam model with varying cross-section area, second moment of inertia, Young's modulus, and structural density. Applying the generalized Euler–Bernoulli beam model instead of more complicated models, e.g., shell model, is common in engineering. Discussions on that are, for instance, given by Forsberg (1969), Trotsenko (2006), and Gavrilyuk et al. (2010) where free (eigen) oscillations of a long axisymmetric structure are considered.

Eigenoscillations of an axisymmetric structure, e.g., shell or beam, are characterized by axisymmetric (if exist) and degenerated (having equal eigenfrequencies) antisymmetric eigenmodes. The degenerated beam-type eigenmodes are not coupled in the linear statement and, normally, define two independent eigenmotions, occurring in two perpendicular planes containing the symmetry axis. For axisymmetric tank shapes, the linear modal sloshing theory (see,Chapters 4 and 5 by Faltinsen and Timokha, 2009, and Appendix A) also distinguishes axisymmetric and degenerated natural sloshing modes. The latter set includes the beam-type sloshing modes consisting of an infinite set of the degenerated pairs whose two elements define mutually ‘perpendicular’ perturbations of the liquid mass center, but axisymmetric and the remaining degenerated natural sloshing modes do not affect the liquid mass center, in the linear approximation. As a consequence,

* Corresponding author. Tel.: +47 73595524.
E-mail addresses: alexander.timokha@ntnu.no, atimokha@gmail.com (A. Timokha).

0889-9746/$ - see front matter
http://dx.doi.org/10.1016/j.jfluidstructs.2013.06.002

'planar' beam vibrations do not perturb the liquid mass center perpendicularly to this plane and, therefore, the coupled tower-linear sloshing motions can independently be considered in the two aforementioned perpendicular planes. The degenerated eigenmodes may be *nonlinearly* coupled due to the so-called internal resonances. The nonlinear phenomena are, however, neglected in the present paper.

Studying the liquid sloshing dynamics implies a description of the hydrodynamic force and moment caused by tower vibrations, and *visa-versa*. One can naturally use Computational Fluid Dynamics (CFD) as exemplified by Curadelli et al. (2010). Other engineering approaches (see,e.g., Shenton and Hampton, 1999; Shrimali and Jangid, 2003; Dutta et al., 2004; Livaoglu and Dogangun, 2007; Livaoglu, 2008; Moslemi et al., 2011) are associated with the so-called equivalent mechanical systems, e.g., pendulum or mass-spring (see more on these phenomenological approaches in the book by Ibrahim, 2005). Adopting the pendulum or/and spring-mass models makes the mathematical modeling less accurate but simpler with respect to CFD. A disadvantage is that the phenomenological modeling may need a set of empirical coefficients and, sometimes, a dedicated experimental validation. An alternative can be the *multimodal method* extensively elaborated by Faltinsen and Timokha (2009). The multimodal method makes it possible to replace, in a rigorous mathematical way, the original sloshing problem by a (modal) system of ordinary differential equations with respect to a set of generalized coordinates $\beta_i(t)$ responsible for the free-surface motions. The right-hand side of these equations depends on the six functions $\eta_n, n=1,\dots,6$ implying the six degrees of freedom of the rigid tank. Lukovsky's formulas express the hydrodynamic force and moment as functions of $\beta_i(t)$ and η_n. These formulas can be used to derive dynamic equations of the entire 'liquid-structure' mechanical system.

The present paper uses the multimodal method and the generalized Euler–Bernoulli beam model to study the coupled eigenoscillations of the considered mechanical system. The original statement is based on the virtual work variational principle (see, Section 2). The statement does not deal with boundary value problems which can be written for this hybrid mechanical system but rather with a four virtual works caused by (i) the force and moment due to the rigid tank inertia, (ii) the inertial force and moment due to beam vibrations, (iii) the force associated the global weight of the structure, and (iv) the hydrodynamic force and moment due to sloshing. The liquid sloshing dynamics is described by using the linear modal equations whose derivation details are theoretically elaborated in chapter 5 by Faltinsen and Timokha (2009). To make the paper self-contained, the required details of the linear modal theory are given in Appendix A.

In Section 3, we derive a differential problem following from the virtual work principle. Mathematically, the problem takes the form of the generalized Euler–Bernoulli beam equation coupled with an infinite-dimensional system of ordinary differential equations with respect to the generalized coordinates describing the natural sloshing modes displacements. The Euler–Bernoulli beam equation are equipped with the clamped end conditions at the lower beam end but the inhomogeneous boundary conditions at the upper end contain, in the right-hand side, the Lukovsky-type modal expressions with respect to the aforementioned generalized coordinates. The expressions imply the resulting hydrodynamic force and moment applied to an axisymmetric rigid tank carrying an ideal incompressible liquid with a free surface. The derived differential problem describes coupled linear free oscillations of the mechanical system.

In Section 5, we use the variational statement for solving the problem on eigenoscillations of the coupled mechanical system. A focus is on the Ritz method and the case of an upright circular cylindrical tank. The method provides a fast convergence and an accurate approximation of the eigensolution. Results are validated by comparing with experiments by Dieterman (1986, 1988). A series of numerical examples demonstrating the dependence of a few lower coupled eigenfrequencies of the mechanical system on the liquid filling is presented.

2. Variational statement of the problem

2.1. Preliminaries

We consider free linear (small-amplitude) oscillations of an axisymmetric tower with an elevated axisymmetric tank installed on the top as shown in Fig. 1. The tank is partly filled by an ideal incompressible liquid with irrotational flow. External force and moment applied to the mechanical system can also be accounted for but the forced motions are not subject of the present study.

The $O_1x_1y_1z_1-$coordinate system is rigidly fixed with the Earth so that O_1z_1 is superposed with the symmetry axis of this multicomponent mechanical system (see, Fig. 1). The tank bottom is rigidly fixed to the tower top so that their symmetry axes coincide with each other. The tower bottom is rigidly clamped to the ground (soil) whose feedback is neglected. As was mentioned in the Introduction, we assume that the tower height is much larger of the tower width (maximum diameter), and one can model the tower oscillations by employing the generalized Euler–Bernoulli beam equation. The beam is characterized by the cross-sectional area S_b, the second moment of inertia $\mathbb{I}$, Young's modulus $\mathbb{E}$ and the mass density ρ_b.

As discussed in the Introduction, linear oscillations of the hybrid axisymmetric mechanical system can be considered as a superposition of beam-type planar eigenoscillations occurring in two perpendicular planes containing the symmetry axis. The planar eigenoscillations are associated with planar motions of the generalized Euler–Bernoulli beam coupled with the hydrodynamic response, force and moment, caused by the 'planar' motions of the beam top. Without loss of generality, the planar beam vibrations are assumed to occur in the $O_1y_1z_1-$plane so that the tank-fixed coordinate system $Oxyz$ is rigidly fixed to the tank top and performs small-amplitude translatory (sway) and angular (roll) motions as shown in Fig. 1. In the linear statement, these motions can be described by instant horizontal displacements of the origin O (because the beam has

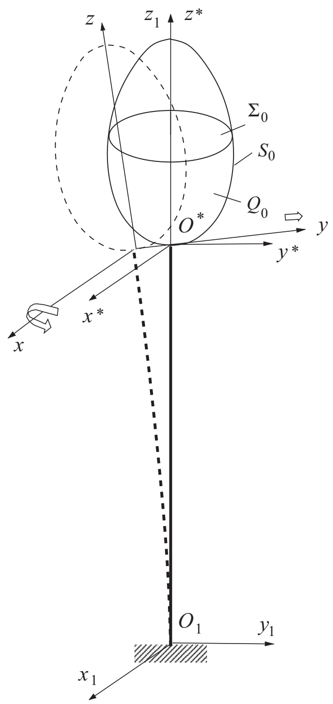

Fig. 1. Main geometric notations. The coordinate system $Oxyz$ is tank-fixed with the origin at the tank bottom. The $O^*x^*y^*z^*$−and $O_1x_1y_1z_1$−coordinate systems are the Earth-fixed ones with O^*z^* and O_1z_1 counterdirected to the gravity acceleration vector **g**.

constant length, vertical displacements are of the second order of smallness with respect to the horizontal displacements), $u(t)$, and instant angular motions, $\vartheta(t)$, of the Oyz-coordinate system around the Ox-axis. The linear modal theory in Appendix A shows that the two degrees of freedom associated with sway, $\eta_2 = u$, and roll, $\eta_4 = \vartheta$, lead to nonzero F_2 (hydrodynamic force in the Oyz-plane) and F_4 (moment around the Ox-axis), but do not cause hydrodynamic loads perpendicular to the Oyz-plane. This means that the liquid mass center remains in the Oyz-plane. Generally speaking, the same is true for the pairs η_1 and η_5 and the hydrodynamic force and moment, F_1 and F_5, respectively, keeping the liquid mass center in the Oxz-plane. Assuming planar motions can fail for the forced resonant excitations leading to the so-called internal resonance and associated *strongly nonlinear* three-dimensional phenomena, e.g., swirling (Gavrilyuk et al., 2000, 2007; Ikeda et al., 2012; Takahara and Kimura, 2012; Faltinsen and Timokha, 2013).

Let $w(z_1, t)$ denote the beam deviations, and l be the beam length (height). Functions $u = \eta_2$ and $\vartheta = \eta_4$ can be expressed in terms of $w(z_1, t)$ and its first-order spatial derivative at $z_1 = l$ as follows:

$$u = w(l, t), \quad \vartheta = -\left.\frac{\partial w}{\partial z_1}\right|_{z_1 = l}. \tag{1}$$

2.2. Virtual work principle

We employ the virtual work variational principle for the Euler beam. According to this principle, the full variation of the beam potential energy (Volmir, 1967)

$$\delta W = \int_0^l \mathbb{EI} \frac{\partial^2 w}{\partial z_1^2} \frac{\partial^2 \delta w}{\partial z_1^2}\, dz_1,$$

where δw are admissible variations of w, should be equal to the sum of virtual works caused, for the linear free oscillations, by inner (with respect to the entire mechanical system) loads applied to the beam, i.e.,

$$\delta W = \sum_{i=1}^{N_f} \delta A_i. \tag{2}$$

Four different inner loads (N_f=4) should be accounted for including (i) the force and moment associated with inertia of the rigid tank body; (ii) the inertial force and moment due to the beam vibration; (iii) the force associated with the weight; (iv) the hydrodynamic force and moment due to sloshing. Furthermore, we give expressions for the virtual works δA_i.

2.3. The virtual works of the non-hydrodynamic nature

By definition, virtual work δA_1 associated with the inertial force and moment associated of the rigid tank body reads as

$$\delta A_1 = -I^{(0)}\ddot{\vartheta}\delta\vartheta + M_t Z_{tC_0}(\ddot{\vartheta}\delta u + \ddot{u}\delta\vartheta) - M_t\ddot{u}\delta u + gM_t Z_{tc_0}\vartheta\delta\vartheta, \tag{3}$$

where g is the gravity acceleration, ρ_t is the tank body density, Q_t is the rigid tank domain, $I^{(0)} = \int_{Q_t}\rho_t(y^2+z^2)\,dQ$ is moment of inertia of the rigid tank around axis Ox, and M_t and $(0,0,Z_{tC_0})$ are the tank body mass and the tank mass center in the $Oxyz$-coordinate system, respectively.

The virtual work δA_2 related to the inertial properties of the beam (tower) is defined as

$$\delta A_2 = -\int_0^l \rho_b S_b \ddot{w}\delta w\, dz_1, \tag{4}$$

where ρ_b is the beam density and S_b is the cross-sectional area of the beam.

The work δA_3 due to the vertical 'weight' force $N(z_1)$ associated with the total beam-and-elevated tank weight (together with liquid) is

$$\delta A_3 = \int_0^l N(z_1)\frac{\partial w}{\partial z_1}\frac{\partial \delta w_1}{\partial z_1}\, dz_1, \tag{5}$$

where

$$N(z_1) = M_0 g + \rho_b S_b g(l - z_1) \tag{6}$$

and $M_0 = M_t + M_l$ is the total mass of the tank body together with the contained liquid.

2.4. The virtual work due to liquid sloshing

This virtual work can be expressed, formally, as

$$\delta A_4 = F_2\delta u + F_4\delta\vartheta, \tag{7}$$

where F_2 is the horizontal hydrodynamic force (in the Earth-fixed coordinate system) along the Oy^* axis and F_4 is the hydrodynamic moment around the Ox^* axis.

The forthcoming analysis needs explicit analytical expressions for F_2 and F_4 as functions of u and ϑ, appearing as disturbances of the rigid tank, and an infinite set of generalized coordinates responsible for the liquid sloshing motions with infinite degrees of freedom. Assuming that the contained liquid is inviscid incompressible with irrotational flow, we adopt the so-called Lukovsky formulas (Lukovsky, 1990; Lukovsky and Timokha, 1995; Faltinsen and Timokha, 2009) for the hydrodynamic force F_2 and moment F_4 as they follow from the linear multimodal method. These formulas contain the aforementioned generalized coordinates which describe the disturbances of the natural sloshing modes.

To make the present paper self-contained, we give some details of the linear modal theory in Appendix A for the most general case, i.e., when the rigid tank motions occur with the six degrees of freedom associated with $\eta_i(t)$, $i=1,\ldots,6$. Appendix A demonstrates that the tank motions in the Oyz plane, here, due to $u=\eta_2$ and $\vartheta=\eta_4$ can lead to the hydrodynamic force F_2 and moment F_4, but keep the liquid mass center in the Oyz plane.

Employing the Lukovsky formula (A.16b) for the horizontal hydrodynamic force F_2 (in the Earth-fixed coordinate system) and the hydrodynamic moment F_4 (formula (A.17a)) rewrites (7) in the form

$$\delta A_5 = \left(-M_l\ddot{u} + M_l Z_{lC_0}\ddot{\vartheta} - \sum_{i=1}^{\infty}\ddot{\beta}_i^s\lambda_i\right)\delta u + \left(M_l Z_{lC_0}\ddot{u} + gM_l Z_{lC_0}\vartheta - J_0^O\ddot{\vartheta} - \sum_{i=1}^{\infty}(\ddot{\beta}_i^s\lambda_{0i}^O + g\beta_i^s\lambda_i)\right)\delta\vartheta, \tag{8}$$

where M_l is the liquid mass and $(0,0,Z_{lC_0})$ is the liquid mass center in the $Oxyz$-coordinate system. Here, (8) introduces the generalized coordinates $\beta_i^s(t)$ describing the free surface elevations in the cylindrical coordinate system associated with $O_{ft}x_{ft}y_{ft}z_{ft}$ and defined by the equation

$$z_{ft} = \sin\,\theta\sum_{i=1}^{\infty}\beta_i^s(t)\varphi_{1,i}(r,0), \tag{9}$$

where $\sin\,\theta\varphi_{1,i}(r,z_{ft})$ are the corresponding natural sloshing modes. The generalized coordinates $\beta_i^s(t)$ are the solution of the modal equations

$$\mu_i(\ddot{\beta}_i^s + \sigma_i^2\beta_i^s) + \lambda_i\left(\ddot{w}(l,t) - g\frac{\partial w(l,t)}{\partial z_1}\right) - \lambda_{0i}^O\frac{\partial \ddot{w}(l,t)}{\partial z_1} = 0, \tag{10}$$

where σ_i are the natural sloshing frequencies but the definition of the hydrodynamic coefficients μ_i, λ_i, $\lambda_{0i}^O = \lambda_{0i} - h\lambda_i$ (h is the liquid depth) and $J_0^O = M_l h(2Z_{lC_0} - h) + J_0$ (the coefficients also appear in (8)) is given in Appendix A by integrals (A.9) and (A.13).

Computing the hydrodynamic coefficients μ_i, λ_i, λ_{0i} and J_0 is a relatively complicated task. Analytical expressions for them exist, e.g., for an upright circular cylindrical tank (Appendix B). Numerical values of the hydrodynamic coefficients for a tapered conical tank are computed by Gavrilyuk et al. (2012). For spherical tanks, the numerical hydrodynamic coefficients can be extracted from supplementary materials of the paper by Faltinsen and Timokha (2013) or based on the analytically approximate natural sloshing modes by Barnyak et al. (2011) and Faltinsen and Timokha (2012).

3. Differential formulation following from the variational principle

When summarizing the five virtual works, variational relation (2) and condition (1) lead together to the variational equation

$$\int_0^l \left[\mathbb{EI}\frac{\partial^2 w}{\partial z_1^2}\frac{\partial^2 \delta w}{\partial z_1^2} - N(z)\frac{\partial w}{\partial z_1}\frac{\partial \delta w}{\partial z_1} + \rho_b S_b \ddot{w}\delta w\right] dz_1 + \left[I^O \frac{\partial \ddot{w}}{\partial z_1}\frac{\partial \delta w}{\partial z_1} + M_0 \ddot{w}\delta w \right.$$
$$\left. + M_0 Z_{C_0}\left(\ddot{w}\frac{\partial \delta w}{\partial z_1} + \frac{\partial \ddot{w}}{\partial z_1}\delta w\right) + \sum_{i=1}^{\infty}\ddot{\beta}_i^s\left(\lambda_i \delta w - \lambda_{0i}^O \frac{\partial \delta w}{\partial z_1}\right) - gM_0 Z_{C_0}\frac{\partial w}{\partial z_1}\frac{\partial \delta w}{\partial z_1} - g\sum_{i=1}^{\infty}\beta_i^s \lambda_i \frac{\partial \delta w}{\partial z_1}\right]_{z_1=l} = 0, \tag{11}$$

where $I^O = I^{(0)} + J_0^O$ is the total (rigid tank plus liquid) inertia moment around the Ox-axis, $M_0 = M_t + M_l$ is the total (tank plus liquid) mass, and Z_{C_0} is the vertical coordinate of the 'tank-liquid' mass center in the $Oxyz$-system, i.e.,

$$Z_{C_0} = \frac{M_t Z_{tC_0} + M_l Z_{lC_0}}{M_t + M_l}. \tag{12}$$

The kinematic constraint is the clamped-end conditions

$$w(0,t) = \frac{\partial w}{\partial z_1}(0,t) = 0 \tag{13}$$

which should be fulfilled for w and δw. Another constraint to (11) is the linear modal system (10).

Integrating by parts (by coordinate z_1) the two first components of (11)

$$\int_0^l \mathbb{EI}\frac{\partial^2 w}{\partial z_1^2}\frac{\partial^2 \delta w}{\partial z_1^2} = \left[\mathbb{EI}\frac{\partial^2 w}{\partial z_1^2}\frac{\partial \delta w}{\partial z_1} - \frac{\partial}{\partial z_1}\left(\mathbb{EI}\frac{\partial^2 w}{\partial z_1^2}\right)\delta w\right]_0^l + \int_0^l \frac{\partial^2}{\partial z_1^2}\left(\mathbb{EI}\frac{\partial^2 w}{\partial z_1^2}\right)\delta w\, dz_1, \tag{14a}$$

$$-\int_0^l N(z)\frac{\partial w}{\partial z_1}\frac{\partial \delta w}{\partial z_1} dz_1 = -\left[N(z_1)\frac{\partial w}{\partial z_1}\delta w\right]_0^l + \int_0^l \frac{\partial}{\partial z_1}\left(N(z_1)\frac{\partial w}{\partial z_1}\right)\delta w\, dz_1 \tag{14b}$$

and using (13) in variational equation (11) fulfilled for arbitrary δw, δw and $\partial \delta w/\partial z_1$ at $z_1 = l$ leads to the following boundary problem with respect to $w(z_1,t)$

$$\frac{\partial^2}{\partial z_1^2}\left(\mathbb{EI}\frac{\partial^2 w}{\partial z_1^2}\right) + \frac{\partial}{\partial z_1}\left(N(z_1)\frac{\partial w}{\partial z_1}\right) + \rho_b S_b \ddot{w} = 0, \quad z_1 \in (0,l), \tag{15a}$$

$$\left[\frac{\partial}{\partial z_1}\left(\mathbb{EI}\frac{\partial^2 w}{\partial z_1^2}\right) + N(z_1)\frac{\partial w}{\partial z_1}\right]_{z_1=l} = \left(M_0\ddot{w} + M_0 Z_{C_0}\frac{\partial \ddot{w}}{\partial z_1}\right)_{z_1=l} + \sum_{i=1}^{\infty}\ddot{\beta}_i^s \lambda_i, \tag{15b}$$

$$\left(\mathbb{EI}\frac{\partial^2 w}{\partial z_1^2}\right)_{z_1=l} = \left(gM_0 Z_{C_0}\frac{\partial w}{\partial z_1} - M_0 Z_{C_0}\ddot{w} - I^O\frac{\partial \ddot{w}}{\partial z_1}\right)_{z_1=l} + \sum_{i=1}^{\infty}\ddot{\beta}_i^s \lambda_{0i}^O + g\sum_{i=1}\beta_i^s \lambda_i, \tag{15c}$$

where $\beta_i^s(t)$ are defined by linear modal equations (10) and the clamped-end conditions (13) are satisfied. The problem should be equipped by the initial conditions at $t = t_0$

$$w(z_1,0) = w_0(z_1), \quad \dot{w}(z_1,0) = w_1(z_1), \quad \beta_i^s(0) = \beta_i^0, \quad \dot{\beta}_i^s(0) = \beta_i^1 \tag{16}$$

to uniquely describe the coupled 'liquid-structure' dynamics.

Eq. (15a) is the generalized Euler–Bernoulli beam equation in the gravity field. A heavy weight is attached to the beam top. The boundary conditions (15b) and (15c) represent the shear force and the bending moment

$$Q = -\left[\frac{\partial}{\partial z_1}\left(\mathbb{EI}\frac{\partial^2 w}{\partial z_1^2}\right) + N(z_1)\frac{\partial w}{\partial z_1}\right] \quad \text{and} \quad M = -\mathbb{EI}\frac{\partial^2 w}{\partial z_1^2},$$

respectively, due to the inner loads applied to the beam top ($z_1 = l$). These loads are caused by the rigid tank motions and the hydrodynamic loads due to the sloshing of the contained liquid.

4. Nondimensional statement

Henceforth, we consider the characteristic length scale R_0 and the characteristic time $\sqrt{R_0/g}$. Then all variables of the problem (15), (10), and (13) as well as the liquid depth can be transformed to the nondimensional form (with overbars)

$$t^2 = \frac{R_0}{g}\bar{t}^2, \quad l = R_0\bar{l}, \quad \lambda_i = \rho_l R_0^3 \bar{\lambda}_i, \quad \sigma_n^2 = \frac{g}{R_0}\bar{\sigma}_n^2, \quad \mu_i = \rho_l R_0^3 \bar{\mu}_i,$$

$$\lambda_{0i}^{O}=\rho_l R_0^4\overline{\lambda}_{0i}^{O},\quad I^O=\rho_l R_0^5\overline{I},\quad \overline{I}=\frac{\rho_t}{\rho_l}I^{(0)}+J_0^O,\quad z_1=R_0\overline{z}_1,$$
$$w=R_0\overline{w},\quad \beta_i^s=R_0\overline{\beta}_i,\quad \mathbb{E}\mathbb{I}=\mathbb{E}_0\mathbb{I}_0\overline{\mathbb{E}\mathbb{I}},\quad N=\frac{\mathbb{E}_0\mathbb{I}_0}{R_0^2}\overline{N},$$
$$\overline{N}=D(\overline{M}_0+\frac{\rho_b}{\rho_l}(\overline{l}-\overline{z}_1)),\quad D=\frac{\rho_l R_0^5 g}{\mathbb{E}_0\mathbb{I}_0},\quad S_b=R_0^2\overline{S}_b,\quad M_0=\rho_l R_0^3\overline{M}_0,$$
$$\overline{M}_0=\left(\frac{\rho_t}{\rho_l}\overline{M}_t+\overline{M}_l\right),\quad Z_{C_0}=R_0\overline{Z}_{C_0},\quad \overline{h}=\frac{h}{R_0},\tag{17}$$

where $\mathbb{E}_0\mathbb{I}_0$ is the bending stiffness in the characteristic cross-section. For brevity, the overbars will furthermore be omitted.

The nondimensional variational equation (11) takes the form

$$\int_0^l\left[\mathbb{E}\mathbb{I}\frac{\partial^2 w}{\partial z_1^2}\frac{\partial^2\delta w}{\partial z_1^2}-N(z_1)\frac{\partial w}{\partial z_1}\frac{\partial\delta w}{\partial z_1}+\frac{\rho_b}{\rho_l}DS_b\frac{\partial^2 w}{\partial t^2}\delta w\right]dz_1+\left\{D\left[I\frac{\partial^3 w}{\partial z_1\partial t^2}\frac{\partial\delta w}{\partial z_1}+M_0Z_{C_0}\left(\frac{\partial^2 w}{\partial t^2}\frac{\partial\delta w}{\partial z_1}+\frac{\partial^3 w}{\partial z_1\partial t^2}\delta w\right)+M_0\frac{\partial^2 w}{\partial t^2}\delta w\right.\right.$$
$$\left.\left.+\sum_{i=1}^{\infty}\ddot{\beta}_i\left(\lambda_i\delta w-\lambda_{0i}^O\frac{\partial\delta w}{\partial z_1}\right)-M_0Z_{C_0}\frac{\partial w}{\partial z_1}\frac{\partial\delta w}{\partial z_1}-\sum_{i=1}^{\infty}\beta_i\lambda_i\frac{\partial\delta w}{\partial z_1}\right]\right\}_{z_1=l}=0,\tag{18}$$

but the nondimensional linear modal equations (10) are

$$\mu_i(\ddot{\beta}_i+\sigma_i^2\beta_i)+\left(\lambda_i\frac{\partial^2 w}{\partial t^2}-\lambda_{0i}^O\frac{\partial^3 w}{\partial z_1\partial t^2}-\lambda_i\frac{\partial w}{\partial z_1}\right)_{z_1=l}=0,\quad i=1,2,\ldots.\tag{19}$$

5. Eigenfrequencies and eigenmodes

5.1. Statement

Eigenoscillations of the mechanical system are associated with the time-harmonic solution

$$w(z_1,t)=\exp(\mathrm{i}\omega t)\mathrm{w}(z_1),\quad \beta_n(t)=\exp(\mathrm{i}\omega t)b_n,\tag{20}$$

which leads to the following spectral boundary problem with respect to unknown spectral parameter ω^2, function $\mathrm{w}(z_1)$, and coefficients $b_i, i=1,2,\ldots$

$$\frac{d^2}{dz_1^2}\left(\mathbb{E}\mathbb{I}\frac{d^2\mathrm{w}}{dz_1^2}\right)+\frac{d}{dz_1}\left(N\frac{d\mathrm{w}}{dz_1}\right)-\omega^2\frac{\rho_b}{\rho_l}DF\mathrm{w}=0,\quad z_1\in(0,l),\tag{21a}$$

$$\left(\mathbb{E}\mathbb{I}\frac{d^2\mathrm{w}}{dz_1^2}\right)_{z_1=l}=\omega^2 D\left[\left(M_0Z_{C_0}\mathrm{w}+I\frac{d\mathrm{w}}{dz_1}\right)_{z_1=l}-\sum_{i=1}^{\infty}b_i\lambda_{0i}^O\right]+DM_0Z_{C_0}\left.\frac{d\mathrm{w}}{dz_1}\right|_{z_1=l}+D\sum_{i=1}^{\infty}b_i\lambda_i,\tag{21b}$$

$$\left[\frac{d}{dz_1}\left(\mathbb{E}\mathbb{I}\frac{d^2\mathrm{w}}{dz_1^2}\right)+N\frac{d\mathrm{w}}{dz_1}\right]_{z_1=l}=-\omega^2 D\left[M_0\left(\mathrm{w}+Z_{C_0}\frac{d\mathrm{w}}{dz_1}\right)_{z_1=l}+\sum_{i=1}^{\infty}b_i\lambda_i\right],\tag{21c}$$

$$\mathrm{w}(0)=\left.\frac{d\mathrm{w}}{dz_1}\right|_{z_1=0}=0,\tag{21d}$$

$$\mu_i(\sigma_i^2-\omega^2)b_i+\left[\omega^2\left(\lambda_{0i}^O\frac{d\mathrm{w}}{dz_1}-\lambda_i\mathrm{w}\right)-\lambda_i\frac{d\mathrm{w}}{dz_1}\right]_{z_1=l}=0.\tag{21e}$$

Substituting (20) into variational equation (18) gives the following variational equation for (21a)–(21c)

$$\int_0^l\left[\mathbb{E}\mathbb{I}\frac{d^2\mathrm{w}}{dz_1^2}\frac{d^2\delta\mathrm{w}}{dz_1^2}-N(z_1)\frac{d\mathrm{w}}{dz_1}\frac{d\delta\mathrm{w}}{dz_1}\right]dz_1-M_0Z_{C_0}D\left(\frac{d\mathrm{w}}{dz_1}\frac{d\delta\mathrm{w}}{dz_1}\right)_{z_1=l}$$
$$-\omega^2 D\int_0^l\frac{\rho_b}{\rho_l}S_b\mathrm{w}\delta\mathrm{w}\,dz_1-\omega^2 D\left[I\frac{d\mathrm{w}}{dz_1}\frac{d\delta\mathrm{w}}{dz_1}+M_0Z_{C_0}\left(\mathrm{w}\frac{d\delta\mathrm{w}}{dz_1}+\frac{d\mathrm{w}}{dz_1}\delta\mathrm{w}\right)\right.$$
$$\left.+M_0\mathrm{w}\delta\mathrm{w}+\sum_{i=1}^{\infty}b_i\left(\lambda_i\delta\mathrm{w}-\lambda_{0i}^O\frac{d\delta\mathrm{w}}{dz_1}\right)\right]_{z_1=l}-D\sum_{i=1}^{\infty}b_i\lambda_i\left.\frac{d\delta\mathrm{w}}{dz_1}\right|_{z_1=l}=0.\tag{22}$$

5.2. Solution method

Solution $\mathrm{w}(z_1)$ of the variational problem (22) is presented in the form

$$\mathrm{w}(z_1)=\sum_{q=1}^{m_0} a_j W_j(z_1), \tag{23}$$

where the coordinate functions W_j satisfy the clamped-end conditions (21d), and a_j are unknown variables.

Because the clamped end conditions (21d) should be *a priori* satisfied for the coordinate functions W_j which must also be complete on the interval $[0,l]$, an appropriate choice of W_j can be

$$W_j(z_1)=z_1^2 P_j\left(\frac{2z_1}{l}-1\right), \tag{24}$$

where $P_j(x)$ are the Legendre polynomials. The polynomials can be computed by using the recurrence relations

$$P_1(x)=1,\quad P_2(x)=x,\quad P_{j+2}(x)=\frac{1}{j+1}[(2j+1)xP_{j+1}(x)-jP_j(x)],$$
$$P'_{j+2}(x)=xP'_{j+1}(x)+(j+1)P_{j+1}(x),\quad P''_{j+2}(x)=xP''_{j+1}(x)+(j+2)P'_{j+1}(x). \tag{25}$$

Substituting (23) into (21e) and (22) (previously multiplying equation (21e) by coefficient D), setting $\delta\mathrm{w}(z_1)=W_i(z_1)$, and truncating (21e) to a finite sum with b_i $(i=1,2,\ldots,n_0)$ gives the spectral matrix problem

$$(A-\omega^2 B)\mathbf{X}=0. \tag{26}$$

Here, the eigenvector $\mathbf{X}$ has coordinates $\{a_1,a_2,\ldots,a_{m_0},b_1,b_2,\ldots,b_{n_0}\}$, elements of symmetric matrices $A=\{\alpha_{ij}\}$ and $B=\{\gamma_{ij}\}$ are defined by the formulas

$$\alpha_{i,j}=\int_0^l\left(\mathbb{EI}\frac{d^2W_j}{dz_1^2}\frac{d^2W_i}{dz_1^2}-N(z_1)\frac{dW_j}{dz_1}\frac{dW_i}{dz_1}\right)dz_1-M_0Z_{C_0}D\left(\frac{dW_j}{dz_1}\frac{dW_i}{dz_1}\right)_{z_1=l},\quad (i,j=1,2,\ldots,m_0),$$
$$\alpha_{i,j+m_0}=-D\lambda_j\left(\frac{dW_i}{dz_1}\right)_{z_1=l},\quad (i=1,2,\ldots,m_0,j=1,2,\ldots,n_0),\alpha_{i+m_0,j+m_0}=D\mu_i\sigma_i^2\delta_{ij},\quad (i,j=1,2,\ldots,n_0),$$
$$\gamma_{i,j}=D\int_0^l\frac{\rho_b}{\rho_l}S_bW_jW_i\,dz_1+D\left[I\frac{dW_j}{dz_1}\frac{dW_i}{dz_1}+M_0Z_{C_0}\left(W_j\frac{dW_i}{dz_1}+\frac{dW_j}{dz_1}W_i\right)+mW_iW_j\right]_{z_1=l},\quad (i,j=1,2,\ldots,m_0),$$
$$\gamma_{i,j+m_0}=D\left(\lambda_jW_i-\lambda_{0j}\frac{dW_i}{dz_1}\right)_{z_1=l},\quad (i=1,2,\ldots,m_0,\ j=1,2,\ldots,n_0),$$
$$\gamma_{i+m_0,j+m_0}=D\mu_i\delta_{ij},\quad (i,j=1,2,\ldots,n_0),$$

where δ_{ij} is the Kronecker delta.

5.3. Convergence

We consider the case of an upright circular cylindrical tank when the hydrodynamic coefficients are taken from Appendix B. The inner tank radius is R_0, r_0 is the beam radius, and δ is the beam wall thickness, $a=r_0/R_0$, $l_1=l/r_0$, and $\delta_1=\delta/r_0$. Accepting R_0 to be the characteristic length scale in (17), the nondimensional area, the constant second moment of inertia, and the coefficient D can be presented as follows:

$$S_b=2\pi a^2\delta_1,\quad \mathbb{I}=\pi a^4\delta_1,\quad D=\frac{D_1}{\pi a^4\delta_1},\quad D_1=\frac{\rho_l g R_0}{\mathbb{E}_0},$$

respectively.

Numerous computational experiments were done to establish a fast convergence. This is demonstrated by the numerical examples in Tables 1 and 2 conducted with neglecting the tank mass, $M_t=0$ $(\rho_t=0)$. The nondimensional values

$$\frac{\rho_b}{\rho_l}=7.8,\quad D_1=0.476\times10^{-7},\quad a=0.5,\quad \delta_1=0.01 \tag{27}$$

(according to (17)) were adopted. The tables show the convergence to nondimensional eigenfrequencies ω_i for $h=1$ and $l_1=20$ versus subdimensions m_0 and n_0 of the vector $\mathbf{X}$. There are two types of nondimensional eigenfrequencies. The first type is caused by liquid sloshing (sloshing-type frequencies) but the second type is associated with the beam vibrations (beam-type frequencies). For the present input data and $n_0\le15$, the beam-type frequencies are $\omega_{n_0+1},\omega_{n_0+2},\ldots$, namely, the first 15 eigenfrequencies (up to ω_{15}) are the sloshing-type frequencies.

5.4. Validation by experiments

Dieterman (1986, 1988) conducted model tests related to our studies. An upright circular cylindrical tank of the radius R_0=0.225 m and the mass M_t=19 kg was filled with the two different liquid depths, $h/R_0=0.5$ and 1.0. The contained liquid was fresh water with $\rho_l=999$ kg/m^3. Other physical and geometric *dimensional* parameters are as follows: the distance Z_{C_0}

by (12) is equal to 0.19 m, moment of inertia of the rigid tank is $I^{(0)}=0.5$ kg m^2, cross-sectional area of the beam $S_b=3.14\times10^{-4}$ m^2, the beam length $l=1.2$ m, $1/(\mathbb{I}_0\mathbb{E}_0)=3.3\times10^{-4}$ (N m^2)$^{-1}$, the tank density is $\rho_t=1190$ kg/m^3, the beam density is $\rho_b=7800$ kg/m^3.

Comparison between the experimental ν_i^* and the theoretical ν_i dimensional frequencies is presented in Table 3. Agreement is satisfactory accounting for small internal structures installed in experimental tank which affect sloshing.

5.5. Lower eigenfrequencies of the system for the weightless tank

Adopting the nondimensional input data (27) and neglecting the tank weight ($M_t=\rho_t=0$), one can get an information on lower nondimensional eigenfrequencies $0<\omega_1<\cdots<\omega_i<\cdots$ and eigenmodes of the mechanical system versus the nondimensional beam length l and the nondimensional liquid depth h (scaled by the tank radius R_0).

Table 1
Convergence to eigenfrequencies ω_i of the entire mechanical system with (27) versus subdimensions m_0 and n_0 of the vector **X**.

m_0	ω_1	ω_2	ω_3	ω_4	ω_{n0+1}	ω_{n0+2}	ω_{n0+3}
$n_0=1$							
3	1.3086905				6.8813844	84.34535	0.0000000
4	1.3086905				6.8813577	84.20592	301.67328
5	1.3086905				6.8813575	84.14868	299.39230
6	1.3086905				6.8813575	84.14739	296.54805
7	1.3086905				6.8813575	84.14727	296.49416
8	1.3086905				6.8813575	84.14727	296.46383
9	1.3086905				6.8813575	84.14727	296.46365
10	1.3086905				6.8813575	84.14727	296.46360
$n_0=2$							
3	1.3086864	2.3069021			6.9330735	84.87793	0.0000000
4	1.3086864	2.3069021			6.9330459	84.73512	305.50586
5	1.3086864	2.3069021			6.9330457	84.67563	303.38190
6	1.3086864	2.3069021			6.9330457	84.67431	300.29854
7	1.3086864	2.3069021			6.9330457	84.67418	300.24745
8	1.3086864	2.3069021			6.9330457	84.67418	300.21354
9	1.3086873	2.3069021			6.9330457	84.67418	300.21336
10	1.3086864	2.3069021			6.9330457	84.67418	300.21330
$n_0=3$							
3	1.3086859	2.3069007	2.9207033		6.9459150	85.03830	0.0000000
4	1.3086859	2.3069007	2.9207033		6.9458872	84.89454	306.55349
5	1.3086859	2.3069007	2.9207033		6.9458870	84.83435	304.47495
6	1.3086859	2.3069007	2.9207033		6.9458870	84.83303	301.32484
7	1.3086863	2.3069007	2.9207032		6.9458870	84.83290	301.27459
8	1.3086864	2.3069007	2.9207032		6.9458870	84.83290	301.23966
9	1.3086864	2.3069006	2.9207032		6.9458870	84.83290	301.23949
10	1.3086864	2.3069006	2.9207032		6.9458870	84.83290	301.23949
$n_0=4$							
3	1.3086858	2.3069004	2.9207026	3.4207562	6.9511865	85.10640	0.0000000
4	1.3086858	2.3069004	2.9207026	3.4207562	6.9511586	84.96226	306.98395
5	1.3086858	2.3069004	2.9207026	3.4207562	6.9511584	84.90177	304.92436
6	1.3086858	2.3069005	2.9207026	3.4207563	6.9511584	84.90045	301.74666
7	1.3086858	2.3069005	2.9207026	3.4207563	6.9511584	84.90032	301.69676
8	1.3086858	2.3069005	2.9207026	3.4207563	6.9511584	84.90032	301.66141
9	1.3086858	2.3069005	2.9207025	3.4207563	6.9511584	84.90032	301.66123
10	1.3086858	2.3069005	2.9207026	3.4207563	6.9511584	84.90032	301.66117

Table 2
Convergence to the beam-type eigenfrequencies $\omega_{n_0+1}, \omega_{n_0+2}$ and ω_{n_0+3} with (27) versus subdimension n_0 with $m_0=10$.

n_0	6	7	8	9	10	11	12	13	14	15
ω_{n0+1}	6.955	6.956	6.957	6.959	6.960	6.960	6.960	6.960	6.961	6.962
ω_{n0+2}	84.96	84.97	84.98	84.98	84.99	84.99	84.99	84.99	85.00	85.00
ω_{n0+3}	302.0	302.1	302.1	302.1	302.2	302.2	302.2	302.2	302.2	302.2

In Fig. 2, we schematically illustrate that the lower ith eigenmode associated with the beam deflection $w_i(z_1)$, $z_1 \in [0, l]$ defined by (23) and the free-surface radial wave profile defined by (9) and (20) as

$$R_b(r) = \sum_{j=1}^{n_0} b_j \varphi_{1,j}(r, 0) = \sum_{j=1}^{n_0} b_j \frac{J_1(k_{1j} r)}{J_1(k_{1j})}$$

is characterized by the monotonic $w_i(z_1)$ (typical for the first eigenmode of the cantilever beam), but the ith radial free-surface profile is mainly determined by the eigenmode $\varphi_{1,i} = J_1(k_{1i} r)/J_1(k_{1i})$.

Fig. 3 analyses differences between the two lowest nondimensional eigenfrequencies ω_1 and ω_2, the nondimensional sloshing frequencies σ_1 and σ_2, and the lowest nondimensional 'beam' eigenfrequency ω_1^* associated with the artificial case when the free surface is covered by a solid plate and no sloshing motions occur. The eigenfrequency ω_1^* can be found from the algebraic system (26) by enforcing $n_0 = 0$. The figure shows how the frequencies change for the fixed nondimensional beam length $l = 15$ when the nondimensional liquid depth varies from 0.2 to 7.0. The solid lines correspond to ω_1 and ω_2, the dashed lines represent the natural sloshing frequencies σ_1 and σ_2 and the dash-and-dotted line implies ω_1^*. Numerical values of the frequencies are presented in Table 4 for $0.2 \le h \le 5.0$

We see in Fig. 3 and Table 4 that, whereas $h < 2$, the eigenfrequencies ω_1 and ω_2 are close to the corresponding natural sloshing frequencies σ_1 and σ_2, respectively. This means that the lower eigenfrequencies of the mechanical system are mainly determined by the liquid sloshing and, as a consequence, $\omega_i \approx \sigma_i, i = 1, 2$, tend to zero in the shallow water limit.

The 'beam' eigenfrequency ω_1^* increases with decreasing liquid depth to become much larger than σ_1 and σ_2. Theoretically, when $h \to 0$, ω_1^* does not tend to infinity but rather to the lowest eigenfrequency of the cantilever beam whose value is far away from the vertical axis interval in Fig. 3.

Fig. 3 demonstrates that increasing the nondimensional liquid depth h makes the lowest nondimensional eigenfrequency ω_1 close to the 'beam' eigenfrequency ω_1^* but the second eigenfrequency ω_2 tends to σ_1. This implies that the lowest and most dangerous eigenfrequency of the mechanical system is almost not affected by liquid sloshing for large tank fillings. From a practical point of view, the lowest eigefrequency can then be replaced by ω_1^* whose computations assume that the tank is completely filled by a liquid (a rigid plate covers the free surface).

The functions $\omega_1 = \omega_1(h, l)$ and $\omega_2 = \omega_2(h, l)$ are shown in Fig. 4 as the corresponding surfaces in the (h, l, ω_i)-space. The solid lines in Fig. 3 are intersections of these surfaces with the vertical plane $l = 15$. The upper plateaus in Fig. 4 are

Table 3
Comparison between the experimental ν_i^* (Hz) and the theoretical ν_i (Hz) dimensional eigenfrequencies. Experiments were conducted by Dieterman (1986, 1988); *err.* is the relative error.

$h/R_0 = 0.5$			$h/R_0 = 1.0$		
ν_i^* (Hz)	ν_i (Hz)	*err.* (%)	ν_i^* (Hz)	ν_i (Hz)	*err.* (%)
1.02	1.065	4.4	1.03	1.07	3.88
1.93	2.088	8.1	1.83	1.84	0.54
2.5	2.472	1.12	–	–	–
3.03	3.077	1.6	–	–	–
3.55	3.597	1.3	–	–	–

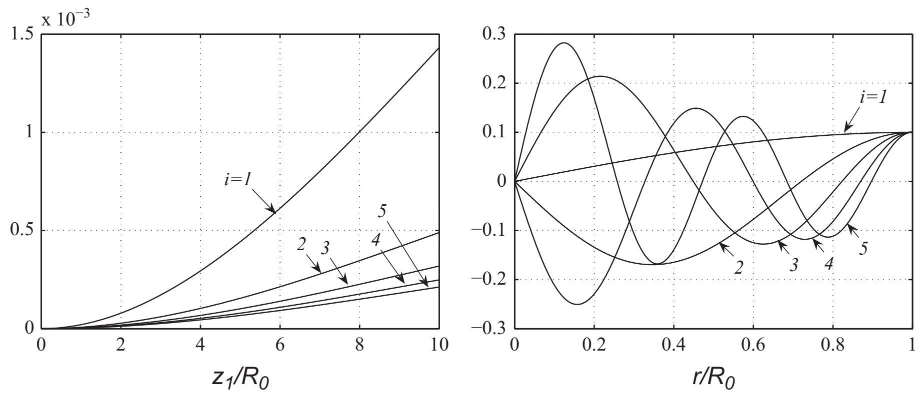

Fig. 2. The enumerated eigenmodes associated with the eigenfrequencies $0 < \omega_1 < \cdots < \omega_i < \cdots$ of the mechanical system. The left panel illustrates the corresponding beam deflections (marked by the i values), but the right panel shows the corresponding radial surface wave profiles. Computations were done with the nondimensional liquid depth $h = 1$ and the nondimensional beam length $l = 10$.

associated with the input parameters (h,l) for which ω_i become close to the corresponding natural sloshing frequencies σ_i with a finite liquid depth. The flat ravine for ω_2 implies the closeness of ω_2 to σ_1, but the lower values of ω_1 appear as $\omega_1 \approx \omega_1^*$. The numerical values of ω_2 steeply change between σ_1 and σ_2 as was already established in Fig. 4 for $l=15$.

6. Concluding remarks

Using the virtual work variational principle, the linear modal sloshing theory by Faltinsen and Timokha (2009) and the Lukovsky formulas for the hydrodynamic force and moment, we examine the free linear (eigen) oscillations of the coupled mechanical system consisting of axisymmetric tower and rigid tank installed at the tower top. The principle derives a boundary problem for the generalized Euler–Bernoulli beam equation coupled with a set of linear ordinary differential equations with respect to generalized coordinates responsible for displacements of the natural sloshing modes. The differential formulation is however not used in our analysis.

Employing the Ritz method and the corresponding variational formulation, we focus on the eigenoscillations of the mechanical system. Numerical experiments demonstrate a fast convergence. Results are validated by Dieterman (1986, 1988)'s experiments. Dependencies of lower eigenfrequencies on the nondimensional liquid depth and the tower height are studied and some practical recommendations are given for lower and higher tank fillings.

The proposed analytical method requires a set of hydrodynamic coefficients which are known for upright circular and annular cylindrical tanks. The literature contains the numerical hydrodynamic coefficients for tapered conical (Gavrilyuk et al., 2012) and spherical (Faltinsen and Timokha, 2013) tanks. Several numerical values of the hydrodynamic coefficients for other axisymmetric tank shapes can be found in the books by Feschenko et al. (1969) and Lukovsky et al. (1984).

The forthcoming studies should concentrate on the forced motions of the coupled mechanical system occurring due to external loads including those caused by earthquake when there appear inhomogeneous kinematic boundary conditions at the tower bottom. Dieterman (1986, 1988) conducted experimental studies on the forced oscillations of the hybrid

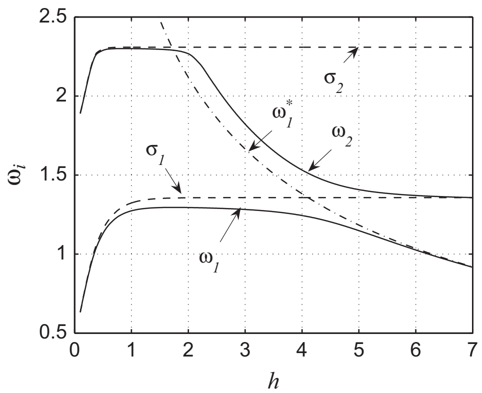

Fig. 3. The nondimensional eigenfrequencies ω_i of the mechanical system, the nondimensional natural sloshing frequencies σ_i and the 'beam' eigenfrequency ω_1^* (the lowest eigenfrequency of the system when the mean free surface is covered by a rigid plate and no sloshing occurs) as functions of the nondimensional liquid depth in an upright circular cylindrical tank. The nondimensional beam length $l=15$.

Table 4
Illustrative numerical values of the nondimensional eigenfrequencies associated with Fig. 3.

h	ω_1	ω_2	σ_1	σ_2	ω_1^*	ω_2^*
0.2	0.8007	2.0454	0.8056	2.0498	5.8171	43.908
0.6	1.1831	2.2972	1.2153	2.3051	3.8676	39.627
1.0	1.2735	2.2999	1.3232	2.3089	3.0533	37.927
1.4	1.2926	2.2969	1.3491	2.3090	2.5742	36.750
1.8	1.2950	2.2867	1.3551	2.3090	2.2477	35.573
2.2	1.2929	2.2046	1.3565	2.3090	2.0060	34.165
2.6	1.2886	1.9985	1.3568	2.3090	1.8173	32.457
3.0	1.2820	1.8219	1.3569	2.3090	1.6645	30.489
3.4	1.2716	1.6826	1.3569	2.3090	1.5374	28.368
3.8	1.2552	1.5748	1.3569	2.3090	1.4295	26.224
4.2	1.2298	1.4951	1.3569	2.3090	1.3364	24.161
4.6	1.1934	1.4411	1.3569	2.3090	1.2551	22.249
5.0	1.1481	1.4076	1.3569	2.3090	1.1833	20.517

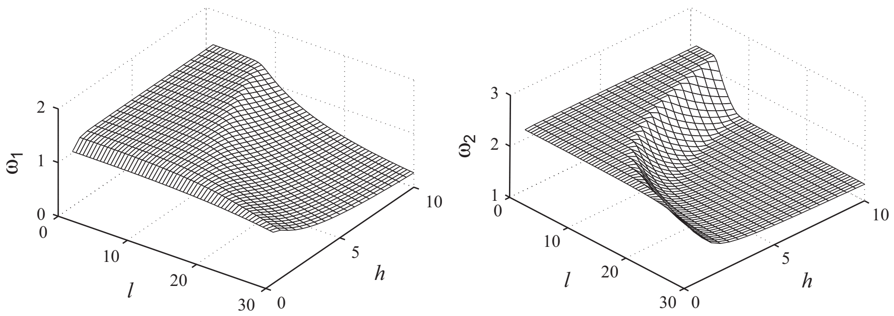

Fig. 4. The two lowest nondimensional eigenfrequencies of the mechanical system versus the nondimensional beam length l and the nondimensional liquid depth h.

mechanical system due to horizontal harmonic excitations. Even though these experimental tests did not establish any three-dimensional motions, the three-dimensional resonant phenomena due to the so-called internal resonances involving the degenerated modes, e.g., swirling, are theoretically possible. Describing them will need a modification of the variational technique as well as the Euler–Bernoulli beam model should probably be revised. Other revisions may be due to internal structures submerged into the liquid (Askari et al., 2012; Takahara et al., 2012).

Employing the multimodal method for other tank shapes and more complicated towers looks theoretically possible. In those cases, the eigenoscillations could be of the three-dimensional nature and, therefore, describing the tower vibrations may need to involve more complicated mathematical models exemplified by Timoshenko's beam, thin-walled shell, or composite structures (Dutta et al., 2004; Gavrilyuk et al., 2010).

Authors thank the German Research Society (DFG) for the financial support.

Appendix A. Elements of the linear modal theory

The linear modal sloshing theory is well known from the 50–60s of the past century. A modern description of the theory is given in Chapter 5 by Faltinsen and Timokha (2009). The theory consists of the linear modal equations and the Lukovsky formulas for the resulting hydrodynamic force and moment. Even though our study needs only particular expressions of this theory, let us outline most general case when an axisymmetric rigid tank moves with six degrees of freedom of a small magnitude as shown in Fig. A1. The liquid is incompressible and ideal with irrotational flows.

Faltinsen and Timokha (2009) constructed the linear modal theory in the $O_{ft}x_{ft}y_{ft}z_{ft}$-coordinate system (see, Fig. A1) rigidly fixed with the tank so that the origin O_{ft} coincides with the geometric center of the mean free surface Σ_0 which belongs to the $O_{ft}x_{ft}y_{ft}$–plane. The mean liquid domain is denoted Q_0 and S_0 is the mean wetted tank surface. The Oz_{ft}-axis is counterdirected to the gravity acceleration vector $\mathbf{g}$ as the tank is at rest. The six degrees of freedom are associated with instant translatory and angular motions of the tank-fixed coordinate system $O_{ft}x_{ft}y_{ft}z_{ft}$ relative to the Earth-fixed coordinate system $O^*x^*y^*z^*$ whose axes are parallel to axes of the $O_1x_1y_1z_1$–system.

We represent the free surface elevations by the Fourier series

$$z_{ft} = \zeta(x_{ft}, y_{ft}, t) = \sum_M \beta_M(t)\varphi_M(x_{ft}, y_{ft}, 0). \tag{A.1}$$

Here, M is, generally speaking, a composite index which may consist of several integer numbers, $\varphi_M(x_{ft}, y_{ft}, z_{ft})$ are the natural sloshing modes, and $\beta_M(t)$ are the generalized coordinates for sloshing motions (modal functions). The natural sloshing modes are eigenfunctions of the spectral boundary problem

$$\nabla^2\varphi_M = 0 \text{ in } Q_0, \quad \frac{\partial\varphi_M}{\partial n} = 0 \text{ on } S_0, \quad \frac{\partial\varphi_M}{\partial n} = \kappa_M\varphi_M \text{ on } \Sigma_0, \quad \int_{\Sigma_0}\varphi_M\, dS = 0, \tag{A.2}$$

where the spectral parameter κ_M determines the natural sloshing frequencies $\sigma_M = \sqrt{g\kappa_M}$ ($g = \|\mathbf{g}\|$), and $\mathbf{n} = (n_1, n_2, n_3)$ is the outer normal.

Using (A.1) and the corresponding modal solution for the velocity potential, Faltinsen and Timokha (2009) derived the following linear ordinary differential (modal)

$$\ddot{\beta}_M + \sigma_M^2\beta_M = K_M t, \tag{A.3}$$

where the right-hand side

$$K_M(t) = -\frac{\lambda_{1M}}{\mu_M}(\ddot{\eta}_{ft1} - g\eta_{ft5}) - \frac{\lambda_{2M}}{\mu_M}(\ddot{\eta}_{ft2} + g\eta_{ft4}) - \frac{\lambda_{01M}}{\mu_M}\ddot{\eta}_{ft4} - \frac{\lambda_{02M}}{\mu_M}\ddot{\eta}_{ft5} - \frac{\lambda_{03M}}{\mu_M}\ddot{\eta}_{ft6} \tag{A.4}$$

involves the hydrodynamic coefficients μ_M, λ_{1M}, λ_{2M} and $\lambda_{0(k-3)M}$ computed via the natural sloshing modes φ_M and the

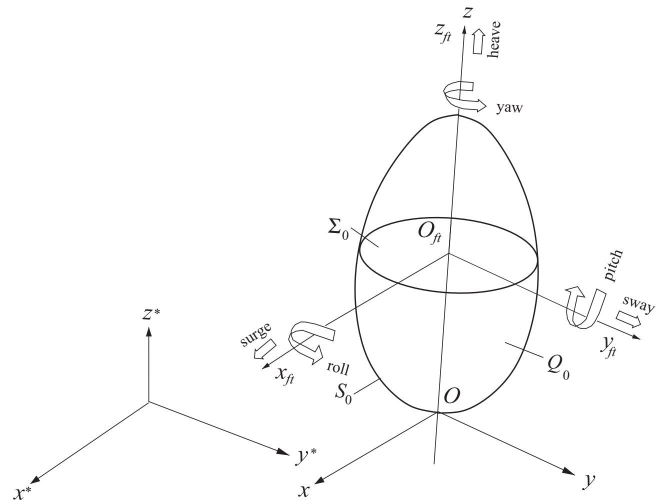

Fig. A1. A general small-amplitude motions of a rigid axisymmetric tank with six degrees of freedom associated with three degrees of freedom for translatory motions (or the tank-fixed coordinate system $O_{ft}x_{ft}y_{ft}z_{ft}$), namely, surge$=\eta_{ft1}(t)$, sway$=\eta_{ft2}(t)$, heave$=\eta_{ft3}(t)$, and angular motions, i.e., roll$=\eta_{ft4}(t)$, pitch$=\eta_{ft5}(t)$, yaw$=\eta_{ft6}(t)$, of the tank. The $O_{ft}x_{ft}y_{ft}z_{ft}$-coordinate system was used by Faltinsen and Timokha (2009) to derive the linear modal equations.

so-called Stokes–Joukowski potentials $\mathbf{\Omega}_0(x_{ft},y_{ft},z_{ft})=(\Omega_{01},\Omega_{02},\Omega_{03})$:

$$\nabla^2\mathbf{\Omega}_0=0 \text{ in } Q_0,\quad \frac{\partial\Omega_{01}}{\partial n}=y_{ft}n_3-z_{ft}n_2,\quad \frac{\partial\Omega_{02}}{\partial n}=z_{ft}n_1-x_{ft}n_3,\quad \frac{\partial\Omega_{03}}{\partial n}=x_{ft}n_2-y_{ft}n_1,\quad \text{on } \Sigma_0\cup S_0. \tag{A.5}$$

Explicit formulas for these hydrodynamic coefficients are as follows:

$$\mu_M=\frac{\rho_l}{\kappa_M}\int_{\Sigma_0}\varphi_M^2\,dS,\quad \lambda_{1\,M}=\rho_l\int_{\Sigma_0}x_{ft}\varphi_M\,dS,\quad \lambda_{2\,M}=\rho_l\int_{\Sigma_0}y_{ft}\varphi_M\,dS,\quad \lambda_{0kM}=\rho_l\int_{\Sigma_0}\varphi_M\Omega_{0k}\,dS,\quad k=1,2,3, \tag{A.6}$$

where, because the liquid is incompressible, ρ_l is the constant liquid density.

Faltinsen and Timokha (2009) also re-derived the linearized Lukovsky formulas for the hydrodynamic force and moment (relative to the origin O_{ft}). The formulas are linear combination of the six degrees of freedom $\eta_{fti}(t)$, the generalized coordinates $\beta_M(t)$ and their second-order derivatives. Coefficients in these formulas are functions of (A.6) and the inertia tensor. For axisymmetric tanks, e.g., upright circular cylindrical, conical, spherical or other tank shapes, both the modal equations and the aforementioned formulas take special form. The reason is that the basic boundary problems (A.2) and (A.5) allow for separation of spatial variables in the cylindrical coordinate system $x_{ft}=r\cos\theta$, $y_{ft}=r\sin\theta$, $z_{ft}=z_{ft}$. The Stokes–Joukowski potentials take then the form

$$\Omega_{01}=-F(r,z_{ft})\sin\theta,\quad \Omega_{02}=F(r,z_{ft})\cos\theta,\quad \Omega_{03}=0, \tag{A.7}$$

where $F(r,z_{ft})$ is the solution of the corresponding boundary-value problem in the meridional plane of Q_0, but the natural sloshing modes are as follows:

$$\varphi_{m,i,1}=\phi_{m,i}(r,z_{ft})\cos(m\theta),\quad \varphi_{m,i,2}=\phi_{m,i}(r,z_{ft})\sin(m\theta),\quad m=0,1,\ldots,\quad i=1,2,\ldots. \tag{A.8}$$

Here, one can detect axisymmetric modes (with $m=0$), but $m\neq0$ implies an infinite set of degenerated modes $\varphi_{m,i,1}$ and $\varphi_{m,i,2}$ corresponding to the same eigenvalue $\kappa_{m,i}$ (natural frequency).

Using (A.7) and (A.8) in (A.6) with the complex index $M=m,i,j$ ($j=1,2$) leads to the following nonzero hydrodynamic coefficients

$$\kappa_i=\kappa_{1,i},\quad \mu_i=\mu_{1,i,1}=\mu_{1,i,2}=\frac{\rho_l\pi}{\kappa_i}\int_{L_0}r\phi_{1,i}^2\,ds,$$
$$\lambda_i=\lambda_{1(1,i,1)}=\lambda_{2(1,i,2)}=\rho_l\pi\int_{L_0}r^2\phi_{1,i}\,ds,\quad \lambda_{0i}=-\lambda_{02(1,i,1)}=\lambda_{01(1,i,2)}=-\rho_l\pi\int_{L_0}r\phi_{1,i}F\,ds, \tag{A.9}$$

where L_0 is the cross-sectional line formed by Σ_0 and the meridional plane. These hydrodynamic coefficients correspond to the so-called beam-type sloshing modes with $m=1$. For other m, the hydrodynamic coefficients are zeros. As a consequence, the modal equations (A.3) with the nonzero right-hand side fall into the two subsets

$$\mu_i(\ddot\beta_i^c+\sigma_i^2\beta_i^c)+\lambda_i(\ddot\eta_{ft1}-g\eta_{ft5})-\lambda_{0i}\ddot\eta_{ft5}=0, \tag{A.10a}$$

$$\mu_i(\ddot\beta_i^s+\sigma_i^2\beta_i^s)+\lambda_i(\ddot\eta_{ft2}+g\eta_{ft4})+\lambda_{0i}\ddot\eta_{ft4}=0, \tag{A.10b}$$

where the modal functions $\beta_i^c(t)$ correspond to the $\cos\theta-$type liquid motions, but $\beta_i^s(t)$ imply the $\sin\theta-$type liquid motions as defined by (A.8); $\sigma_i^2 = g\kappa_i$. The remaining generalized coordinates corresponding to the sloshing modes with $m\neq 1$ are described by the linear homogeneous oscillator equations. These generalized coordinates do not depend on the tank motions and can be nonzeros exclusively due to initial perturbations. This means that the only beam-type linear sloshing modes are directly excited so that $\beta_i^c(t)$ depend on excitations in the $O_{ft}x_{ft}z_{ft}$ plane, η_{ft1} and η_{ft5}, but $\beta_i^s(t)$ are independently excited by η_{ft2} and η_{ft4} implying the tank motions in the $O_{ft}y_{ft}z_{ft}$ plane.

Another component of the linear modal theory is the so-called linearized Lukovsky formulas for the hydrodynamic force. Based on derivations in Faltinsen and Timokha (2009), the force $\mathbf{F}_{O_{ft}} = (F_1^{O_{ft}}, F_2^{O_{ft}}, F_3^{O_{ft}})$ and the moment $\mathbf{M}_{O_{ft}} = (F_4^{O_{ft}}, F_5^{O_{ft}}, F_6^{O_{ft}})$ (projections in the $O_{ft}x_{ft}y_{ft}z_{ft}-$coordinate system) take the form

$$F_1^{O_{ft}} = M_l(g\eta_{ft5} - \ddot{\eta}_{ft1} - z_{lC_0}\ddot{\eta}_{ft5}) - \sum_{i=1}^{\infty}\lambda_i\ddot{\beta}_i^c,$$
$$F_2^{O_{ft}} = M_l(-g\eta_{ft4} - \ddot{\eta}_{ft2} + z_{lC_0}\ddot{\eta}_{ft4}) - \sum_{i=1}^{\infty}\lambda_i\ddot{\beta}_i^s, \quad F_3^{O_{ft}} = -M_l g\ddot{\eta}_{ft3}, \tag{A.11}$$

and

$$F_4^{O_{ft}} = M_l z_{lC_0}(g\eta_{ft4} + \ddot{\eta}_{ft2}) - J_0\ddot{\eta}_{ft4} - \sum_{i=1}^{\infty}(g\lambda_i\beta_i^s + \lambda_{0i}\ddot{\beta}_i^s),$$
$$F_5^{O_{ft}} = M_l z_{lC_0}(g\eta_{ft5} - \ddot{\eta}_{ft1}) - J_0\ddot{\eta}_{ft5} + \sum_{i=1}^{\infty}(g\lambda_i\beta_i^c + \lambda_{0i}\ddot{\beta}_i^c), \quad F_6^{O_{ft}} = 0, \tag{A.12}$$

respectively. Here, M_l is the liquid mass

$$J_{011} = J_{022} = J_0 = \rho_l\pi\int_{L_0+L_1} F\frac{\partial F}{\partial n}\,ds \tag{A.13}$$

(L_1 is the cross-sectional line formed by S_0 and the meridional plane) are the only two nonzero elements (for an axisymmetric tank)

$$J_{0ij} = \rho_l\int_{\Sigma_0\cup S_0}\Omega_{0i}\frac{\partial\Omega_{0j}}{\partial n}\,dS,$$

and $\mathbf{r}_{lC_0} = (0, 0, z_{lC_0})$ is the mass center of the unperturbed liquid in the $O_{ft}x_{ft}y_{ft}z_{ft}-$system.

Expressions (A.11) and (A.12) show that only the beam-type sloshing modes associated with the generalized coordinates $\beta_i^c(t)$ and $\beta_i^s(t)$ effect the liquid mass center and, thereby, the hydrodynamic force and moment. Furthermore, it is important for the present study, that the tank motions in the $O_{ft}y_{ft}z_{ft}$ plane, η_{ft2} and η_{ft4}, lead to nonzero hydrodynamic loads in this plane, F_2 and F_4, but do not cause the force and moment component perpendicular to $O_{ft}y_{ft}z_{ft}$. The same is true for the $O_{ft}x_{ft}z_{ft}$ plane and the pairs η_{ft1}, η_{ft5} and F_1, F_5.

In the present paper, the hydrodynamic force and moment are considered in the $Oxyz$-coordinate system whose three-dimensional translatory and angular motions are defined by the six generalized coordinates $\eta_i,\ i = 1, \dots, 6$ connected with $\eta_{fti},\ i = 1, \dots, 6$ by formulas

$$\eta_{ft1} = \eta_1 + h\eta_5, \quad \eta_{ft2} = \eta_2 - h\eta_4, \quad \eta_{ft3} = \eta_3, \quad \eta_{ft4} = \eta_4, \quad \eta_{ft5} = \eta_5, \quad \eta_{ft6} = \eta_6 \tag{A.14}$$

so that the modal equations (A.10) take the form

$$\mu_i(\ddot{\beta}_i^c + \sigma_i^2\beta_i^c) + \lambda_i(\ddot{\eta}_1 - g\eta_5) - \lambda_{0i}^O\ddot{\eta}_5 = 0, \tag{A.15a}$$

$$\mu_i(\ddot{\beta}_i^s + \sigma_i^2\beta_i^s) + \lambda_i(\ddot{\eta}_2 + g\eta_4) + \lambda_{0i}^O\ddot{\eta}_4 = 0, \tag{A.15b}$$

where $\lambda_{0i}^O = \lambda_{0i} - h\lambda_i$.

The hydrodynamic force components are then computed by

$$F_1 = [M_l g\eta_5] + M_l(-\ddot{\eta}_1 - Z_{lC_0}\ddot{\eta}_5) - \sum_{i=1}^{\infty}\lambda_i\ddot{\beta}_i^c, \tag{A.16a}$$

$$F_2 = [-M_l g\eta_4] + M_l(-\dot{\eta}_2 + Z_{lC_0}\ddot{\eta}_4) - \sum_{i=1}^{\infty}\lambda_i\ddot{\beta}_i^s, \quad F_3 = -M_l g\ddot{\eta}_3 \tag{A.16b}$$

where $Z_{lC_0} = h + z_{lC_0}$ (h is the mean liquid depth) is the vertical coordinate of the mass center in the $Oxyz$-coordinate system, and the square-brackets terms are yielded by the liquid weight considered in the mobile coordinate system $Oxyz$. To get projections of the hydrodynamic force on the $O^*x^*y^*z^*-$axes, the square-brackets terms should be omitted.

The hydrodynamic moments relative to O are defined by the formula $\mathbf{M}_O = \mathbf{r}_{OO_{ft}} \times \mathbf{F}_{O_{ft}} + \mathbf{M}_{O_{ft}}$, where $\mathbf{r}_{OO_{ft}}$ is the radius-vector of O_{ft} with respect to O. According to definitions in Fig. A1, the two nonzero components of $\mathbf{M}_O = (F_4, F_5, 0)$ are

$$F_4 = M_l Z_{lC_0}[g\eta_4 + \ddot{\eta}_2] - J_0^O\ddot{\eta}_4 - \sum_{i=1}^{\infty}(g\lambda_i\beta_i^s + \lambda_{0i}^O\ddot{\beta}_i^s), \tag{A.17a}$$

$$F_5 = M_l Z_{lC_0}[g\eta_5 - \ddot{\eta}_1] - J_0^O \ddot{\eta}_5 + \sum_{i=1}^{\infty} (g\lambda_i \beta_i^c + \lambda_{0i}^O \ddot{\beta}_i^c), \tag{A.17b}$$

where $J_0^O = M_l h(2Z_{lC_0} - h) + J_0$ is the nonzero inertia tensor component defined relative to O (J_0 is defined relative to O_{ft}). The formula for J_0^O can be obtained by direct derivations, or, alternatively, by Steiner's theorem (see,discussion of this theorem in Chapter 5 by Faltinsen and Timokha, 2009).

In our analysis, since we concentrate on the tank motions in the Oyz plane shown in Fig. 1, we will need expressions for the hydrodynamic force (A.16b) and moment (A.17a). The perpendicular hydrodynamic loads are not excited by the degrees of freedom η_2 and η_4.

Appendix B. Hydrodynamic coefficients for an upright circular cylindrical tank

When an upright rigid circular cylindrical tank has the radius R_0, section 5.4.4 by Faltinsen and Timokha (2009) gives the required hydrodynamic coefficients as

$$\sigma_j^2 = \frac{g\zeta_j \tanh(\zeta_j h/R_0)}{R_0}, \quad \mu_j = \frac{\rho_l \pi R_0^3(\zeta_j^2 - 1)}{2\zeta_j^3 \tanh(\zeta_j h/R_0)}, \quad \lambda_j = \frac{\rho_l \pi R_0^3}{\zeta_j^2}, \quad \lambda_{0j} = \frac{2\pi\rho_l R_0^4}{\zeta_j^3} \tanh\left(\frac{\zeta_j h}{2R_0}\right),$$

$$J_0 = J_0^O = \rho_l \pi R_0^2 \left[\frac{1}{3}h^3 - \frac{3}{4}hR_0^2 + 16R_0^3 \sum_{j=1}^{\infty} \frac{\tanh(\zeta_j h/(2R_0))}{\zeta_j^3(\zeta_j^2 - 1)}\right],$$

where ζ_j are the enumerated (in ascending order) roots of equation $J'_1(\zeta_j) = 0$ (J_1 is the Bessel function of the first kind).

References

Askari, E., Daneshmand, F., Amabili, M., 2012. Coupled vibrations of a partially fluid-filled cylindrical container with an internal body including the effect of free surface waves. Journal of Fluids and Structures 27 (7), 1049–1067.

Barnyak, M., Gavrilyuk, I., Hermann, M., Timokha, A., 2011. Analytical velocity potentials in cells with a rigid spherical wall. Zeitschrift für Angewandte Mathematik und Mechanik 91 (1), 38–45.

Curadelli, O., Ambrosini, D., Mirasso, A., Amani, M., 2010. Resonant frequencies in an elevated spherical container partially filled with water: FEM and measurement. Journal of Fluids and Structures 26 (1), 148–159.

Dieterman, H., 1986. An analytically derived lumped-impendance model for the dynamic behaviour of a watertower. Ingenieur–Archiv 56, 265–280.

Dieterman, H., 1988. Dynamics of Towers. Liquid–Structure–Foundation Interaction. Ph.D. Thesis. Technical University Delft.

Dutta, S., Mandal, A., Dutta, S., 2004. Soil-structure interaction in dynamic behavior of elevated tanks with alternate frame staging configurations. Journal of Sound and Vibration 277, 825–853.

Faltinsen, O., Timokha, A., 2009. Sloshing. Cambridge University Press, Cambridge.

Faltinsen, O., Timokha, A., 2012. Analytically approximate natural sloshing modes for a spherical tank shape. Journal of Fluid Mechanics 703, 391–401.

Faltinsen, O., Timokha, A., 2013. Multimodal analysis of weakly nonlinear sloshing in a spherical tank. Journal of Fluid Mechanics 719, 129–164.

Feschenko, S., Lukovsky, I., Rabinovich, B., Dokuchaev, L., 1969. Methods of determining the added liquid mass in mobile cavities. Naukova Dumka Kiev (in Russian).

Forsberg, K., 1969. Axisymmetric and beam-type vibrations of thin cylindrical shells. AIAA Journal 7 (2), 221–227.

Gavrilyuk, I., Hermann, M., Lukovsky, I., Solodun, O., Timokha, A., 2012. Multimodal method for linear liquid sloshing in a rigid tapered conical tank. Engineering Computations 29 (2), 198–220.

Gavrilyuk, I., Hermann, M., Trotsenko, Y., Timokha, A., 2010. Eigenoscillations of three- and two-element flexible systems. International Journal of Solids and Structures 47, 1857–1870.

Gavrilyuk, I., Lukovsky, I., Timokha, A.N., 2000. A multimodal approach to nonlinear sloshing in a circular cylindrical tank. Hybrid Methods in Engineering 2 (4), 463–483.

Gavrilyuk, I., Lukovsky, I., Trotsenko, Y., Timokha, A., 2007. Sloshing in a vertical circular cylindrical tank with an annular baffle. Part 2. Nonlinear resonant waves. Journal of Engineering Mathematics 57, 57–78.

Ibrahim, R., 2005. Liquid Sloshing Dynamics. Cambridge University Press.

Ikeda, T., Ibrahim, R., Harata, Y., Kuriyama, T., 2012. Nonlinear liquid sloshing in a square tank subjected to obliquely horizontal excitation. Journal of Fluid Mechanics 700, 304–328.

Livaoglu, R., 2008. Investigation of seismic behavior of fluid-rectangular tank-soil/foundation systems in frequency domain. Soil Dynamics and Earthquake Engineering 28, 132–146.

Livaoglu, R., Dogangun, A., 2007. Effect of foundation embedment on seismic behavior of elevated tanks considering fluid-structure-soil interaction. Soil Dynamics and Earthquake Engineering 27, 855–863.

Lukovsky, I., 1990. Introduction to Nonlinear Dynamics of Rigid Bodies with the Cavities Partially Filled by a Fluid. Naukova Dumka, Kiev in Russian.

Lukovsky, I., Timokha, A., 1995. Variational Methods in Nonlinear Problems of the Dynamics of a Limited Liquid Volume. Institute of Mathematics of NASU in Russian.

Lukovsky, I.A., Barnyak, M.Y., Komarenko, A.N., 1984. Approximate Methods of Solving the Problems of the Dynamics of a Limited Liquid Volume. Naukova Dumka, Kiev in Russian.

Moslemi, M., Kianoush, M., Pogorzelski, W., 2011. Seismic response of liquid-filled elevated tanks. Engineering Structures 33, 2074–2084.

Shenton, H., Hampton, F., 1999. Seismic response of isolated elevated water tanks. Journal of Structural Engineering 125, 965–976.

Shrimali, M., Jangid, R., 2003. Earthquake response of isolated elevated liquid storage steel tanks. Journal of Constructional Steel Research 59, 1267–1288.

Takahara, H., Hara, K., Ishida, T., 2012. Nonlinear liquid oscillation in a cylindrical tank with an eccentric core barrel. Journal of Fluids and Structures 35, 120–132.

Takahara, H., Kimura, K., 2012. Frequency response of sloshing in an annular cylindrical tank subjected to pitching excitation. Journal of Sound and Vibration 331 (13), 3199–3212.

Trotsenko, Y., 2006. Frequencies and modes of vibration of a cylindrical shell with attached rigid body. Journal of Sound and Vibration 292, 535–551.

Volmir, A., 1967. Stability of Deformable Systems. Nauka, Moscow.